Food Anal. Methods (2015) 8:2150–2156
DOI 10.1007/s12161-015-0109-7

# Qualitative Identification of Fish Meal and Meat Bone Meal via Fluorescence Spectral Imaging

**Yuanpeng Li · Furong Huang · Ruiyi Xian · Xiaoshu Lu · Jia Dong · Zhenqiang Chen · Yong Wang · Xingdan Chen**

Received: 24 October 2014 / Accepted: 22 January 2015 / Published online: 4 February 2015


**Abstract** In order to improve feed safety, we investigated the feasibility of using fluorescence spectral imaging (FSI) technique to qualitatively detect meat and bone meal (MBM) mixed with fish meal (FM). Using the FSI system, the spectra of 90 FM and MBM samples from different regions were collected with denoising and binary processing to obtain images. The spectral data curves over the wavelength range of 400–680 nm were used for identification and were pre-treated with various methods. Next, the curves were plotted based on stereo spectrograms; then, partial least squares discriminant analysis (PLS-DA) was applied to determine the FM and MBM samples. One FM sample and one MBM sample were randomly selected and mixed together (*v*/*v*, 1:1), and the mixture's pseudo-color (PC) image was generated by mapping the best grayscale values using a spectrogram method. The resulting PC image was then used for spatial identification of the mixture. The PLS-DA results indicated that the identification effect was best after the multiplicative scatter correction where the sensitivity, specificity, and accuracy all equaled to 1. The PC image demonstrate that the FM (green) and MBM (red) accounted for 52.6 and 47.4 % of the total volume, respectively, corresponding with the actual 1:1 ratio. Additionally, the experimental test of three low concentration-mixed powder samples (c[MBM]=1.5 %, c[MBM]=3 %, and c[MBM]=5 %) determined that the lower limit of application (LLA) of the proposed method is c[MBM]=1.5 %. Theoretical limit of detection (LOD) of the method was calculated about c[MBM]=0.75 % through linear regression. These experiments show that the spectral and spatial information provided by FSI can rapidly and nondestructively determine whether FM is mixed with MBM.

**Keywords** Inflorescence spectral imaging · Partial least squares discriminant analysis · Fish meal · Meat and bone meal · Pseudo-color image · Identification

Y. Li · F. Huang (✉) · R. Xian · X. Lu · J. Dong · Z. Chen · X. Chen
Department of Opto-Electronic Engineering, Jinan University, Guangzhou 510632, China
e-mail: furong_huang@163.com

X. Chen
Changchun Institute of Optics, Fine Mechanics and Physics, Chinese Academy of Sciences, Changchun 130033, China

Y. Wang
Department of Food Science and Engineering, Jinan University, Guangzhou 510632, China

## Introduction

Fish meal (FM) is a nutrient-rich, high-protein supplemental feed ingredient that is used primarily in diets for domestic animals and farmed fish (Wang et al. 2012). FM's protein digestion rate is as high as 90 % with a balanced amino acid composition high in both lysine and methionine. FM is also rich in minerals and vitamins with proper calcium and phosphorous ratios, making it a highly utilized product. For these reasons, FM plays an important role in aquaculture diets (Yang 2010); but the scarcity and high demand of fishery resources drive the inflation of FM products. Some businessmen mix FM with cheap, low-protein meat and bone meal (MBM) illegally. According to the research, the bovine spongiform encephalopathy (BSE), commonly known as mad cow disease, is caused by prions contained in the MBM fed to the cattle. In 2001, China announced a law to prohibit the use of the animal-based protein supplement because not only does MBM reduce FM quality but also affects the

absorption of other nutrients. More seriously, MBM carrying BSE virus may transmit the disease to animals feeding on the diet, threatening the health of those animals as well as consumers. For these reasons, developing new methods to identify MBM mixed in FM rapidly and conveniently will ensure the safe use of FM.

According to the literature, current approaches for FM and MBM detection include sensory evaluation (Chen. 2003; Yang et al. 2006), microscopy analysis (Zhang et al. 2009), enzyme-linked immunosorbent assay (ELISA) (Liu 2006), polymerase chain reaction (PCR) (Cao et al. 2003), and near infrared spectroscopy (NIR) (Lv et al. 2013; Zhan et al. 2009; Shi et al. 2009). Each of the above methods has its own advantages and disadvantages. For example, sensory evaluation requires highly qualified and experienced inspectors who are subjective by nature. Microscopy analysis has a low detection limit and good thermal stability, but these analyses require skilled technicians, who can distinguish the morphology of plant and animal particles. ELISAs recognize specific antigens with low costs and are suitable for liquid samples; however, results may be distorted by products of ruminant animals such as milk and gelatin. Additionally, ELISAs are sensitive to high temperature and shows cross reactivity with plant proteins. PCR methods can identify specific DNA sequences, but they can be expensive. NIR provides rapid, nondestructive detection and is suitable for quantitative analysis; however, calibration requires massive amounts of data and the detection limit is high. Due to the limitations of these methods, techniques must improve and overcome their technical limitations or new detection methods need to be developed.

Commonly used protein feeds give various fluorescence responses carrying a large amount of useful physical and chemical information. The stronger the fluorescence is, the more accurate the identification is. While this is not suitable for protein feed that does not fluoresce, both FM and MBM give distinct fluorescence signals, so it is possible for them to be distinguished using fluorescence spectral imaging (FSI).

In this study, we investigated the feasibility of using the spectral and spatial information provided by FSI to identify FM and MBM qualitatively. Spectral imaging has been widely applied since its discovery in various fields, such as food science (Zhu et al. 2013; Peng et al. 2010), traditional Chinese drug detection (Hang et al. 2010; Zhao et al. 2010), medical molecular biology (Gendrin et al. 2007), and immunofluorescent medicine (Constantinou et al. 2009). FSI refers to a technique in which images are collected, displayed, processed, and analyzed through multiple spectral channels. Some advantages include low amounts of sample requirement, high sensitivity, and nondestructive, real-time dynamic detection.

The spectral information provided here to detect FM and MBM levels by FSI was combined with partial least squares discriminant analysis (PLS-DA), a discriminant analysis method based on PLS regression. The information of a class member is provided by the auxiliary matrix as codes and is taken into account while setting up the factors; therefore, the technique has high identification ability (Hao et al. 2010; Heinzmann et al. 2010). The application of PLS-DA allows small differences between samples to be distinguished. We also used FSI on a 1:1 mixture of FM/MBM using a grayscale histogram distribution to map the pseudo-color (PC) image which was then used for spatial determination of whether FM was mixed with MBM.

Based on the spectral and spatial information provided by the FSI technique, we established a model for fast identification of MBM mixed in FM through the PLS-DA method. The spatial distribution of the FM and MBM mixture was determined through imaging, and the feasibility of applying FSI to the identification of FM and MBM was investigated. The study provides a rapid method of detecting MBM hidden in FM.

## Experiment

### Equipment

The experiment adopted a staring type FSI device designed and developed by the Laboratory of Optoelectronic Information and Sensing Technology at Jinan University. The core components include a UV light source whose central wavelength is 254 nm, an interference filter, a VariSpec liquid crystal tunable filter (LCTF) controller, a charge-coupled device (CCD) camera, a set of lenses, a video capture card, and a computer (Fig. 1). Figure 2 shows the acquisition process for

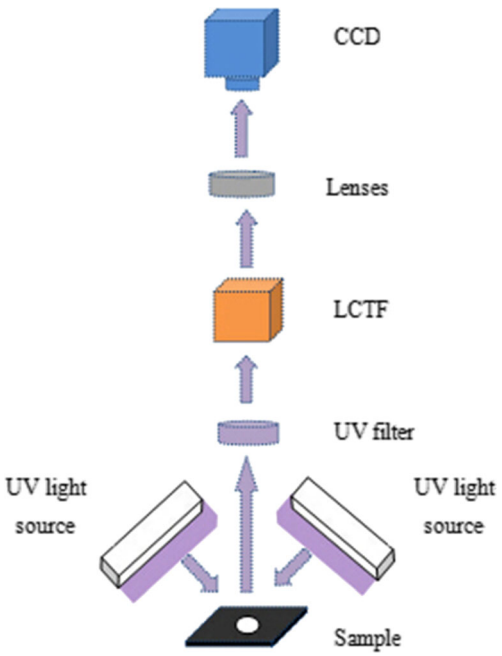


**Fig. 1** Schematic diagram of the experimental device

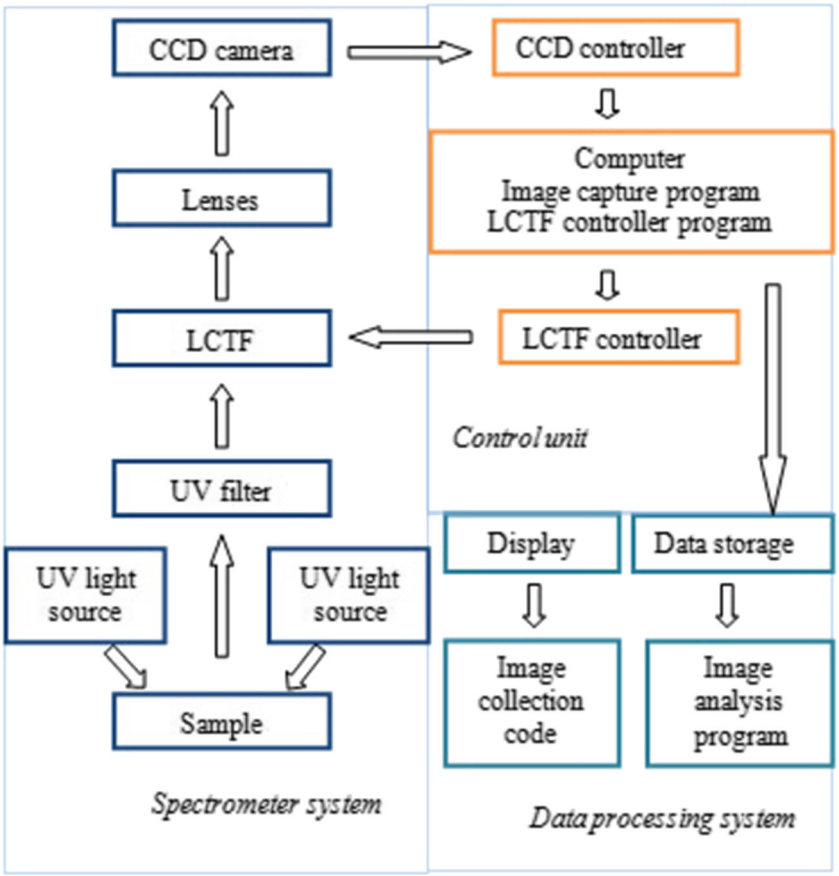


**Fig. 2** The acquisition process of fluorescence spectral images

obtaining fluorescence spectral images. To test the equipment, a sample was placed on the stage and fluorescence emission was observed upon UV excitation. The emitted light was divided by the LCTF controller, and the final image was captured using a CCD camera and recorded in the computer.

## Sample Preparation

In the present study, we analyzed various FM and MBM samples gathered from different regions. There were 50 FM sample collected including Peruvian steam-dried FM, red FM from Tasha Peru, Shandong non-fat FM, Dongguan steam FM, and Beihai FM. We also used 40 MBM samples including Uruguayan MBM, Australian MBM, Henan MBM, and Beijing MBM. All 90 samples were passed through a standard 50-mesh sieve, bagged and marked. To prepare a mixed powder, one FM sample and one MBM sample were randomly selected and 1 g of each was weighed and put into a new sample bag.

## Image and Spectrum Acquisition

To reduce the external light interference, the acquisition process was performed in a darkroom. All 90 FM and MBM samples were tested using the spectral imaging system recording data every 5 nm along the 450–680-nm wavelength range. The CCD converts optical signals into electrical signals, recording them in a computer through the video capture card. Each detection generated a spectral cube of the sample consisting of 47 frame, 256 grayscale images.

These spectral images carry the physical structure, chemical composition, and the morphology of the FM and MBM sample. Background, noise, and other interference that complex or conceal the information of tested samples under certain conditions must be corrected for; therefore, it is necessary to perform image denoising and binary treatment to eliminate inevitable noise, to reduce the effect of external factors, and to simplify the calculations to obtained data during the imaging process. After determining the effective pixel, the statistical average was generated to get the spectrum intensity curve.

## The Principle of the Grayscale Histogram Threshold Segmentation Method

Thresholding is the most common parallel regional technology and is the simplest method of image segmentation (Castlcman 1998). The peaks, valleys, and curvatures of the histogram were used to categorize whether each was a single-peak histogram, double-peak histogram, or multiple-peak histogram, and the proper thresholding method was then selected

accordingly. Images with multiple objects and backgrounds can be seen in grayscale histograms corresponding to multiple peaks and valleys containing less edge. This histogram technique was used to determine the threshold of such an image.

The grayscale threshold, $T$, was used to calculate the object area by the following formula:

$$A = \int_{T}^{\infty} H(D)dD \quad (1)$$

As shown in the formula, the change of threshold from $T$ to $T+\Delta T$ has a very small effect on the area; so, using the peaks and valleys as the threshold can minimize the measurement error of area. For an image with multiple objects and large differences in background, choosing several grayscale thresholds based on the histogram can reduce the effect of small mistakes made during the area selection, providing effective segmentation of the background and multiple objects (Zhang 1998; Yang 2006).

## Results and Discussion

### Image and Spectrum Analysis

A cube consisting of 47 frames and 256 grayscale images was generated for each sample after spectral imaging. Figure 3 is the fluorescence image of FM samples at 560 nm and Fig. 4 shows the binary image.

The average spectrum curves of FM and MBM were plotted based on the spectral cubes (Fig. 5). The spectrum curves of FM and MBM had the same trend over the wavelength range of 400–680 nm and their peaks and valleys were synchronous. The fluorescence intensity of FM was higher than that of MBM. These results implicate that the average spectrum curves of FM and MBM are suitable for primary detection, but to make the results more intuitive and accurate, we further processed the spectral data using the information obtained from FSI combined with the PLS-DA method. We found that the FM and MBM samples were identified reliably and accurately and that the spatial distribution of the mixed powder could be obtained by imaging.

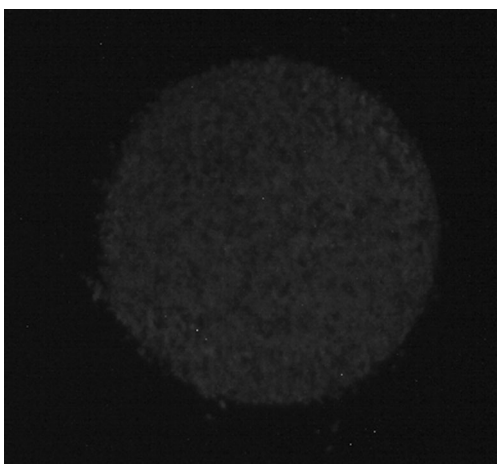

**Fig. 3** Fluorescence images of fish meal at 560 nm

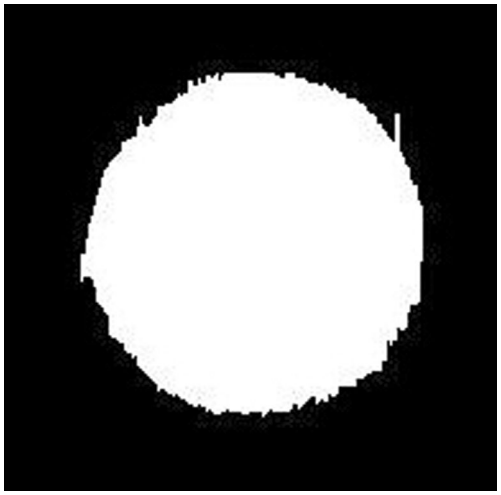

**Fig. 4** Binary images of fish meal at 560 nm

### Identification Using the PLS-DA Model

PLS-DA is the most commonly used chemometric method, and it is a categorical technique based on PLS. It gathers categorical information according to sample features and establishes a regression model between the independent and categorical variables to efficiently extract the characteristic variables related to classification (Ouyang and Zhao 2013).

The PLS-DA model created for this study is a regression-discriminant model of sample categorical variables and fluorescent spectra according to the samples' actual categorical features. During the process, variable classification was assigned based on the fluorescence spectral features of FM

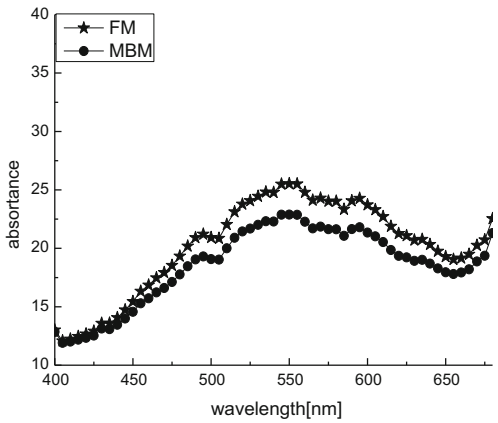


**Fig. 5** Average spectrum curves of fish meat and meat and bone meal

and MBM. Ninety samples were randomly distributed to the calibration set containing 70 samples or the prediction set for the remaining 20 samples.

The PLS-DA MATLAB Version 2.0 program, designed by Professor Yi Liang in the Modern Research Center of Traditional Chinese Medicine at Central South University, was used for the main process of discriminant analysis including data input, determining the principal component number based on the cross-verification misclassification rate, establishing the discriminant model of optimal component scores, plotting the PLS-DA score scatter diagram, and prediction of the predicted samples.

In discriminant analysis, the critical factors determining whether the analysis is successful are the selection and pretreatment of the data. To get rid of the influence of heterogeneous samples and light scattering, the original data was pre-treated with first derivative, second derivative, multiple scatter correction, and standard normal transformation. The resulting data was processed with PLS-DA to compare the effects of different pretreatment methods on discriminant analysis (Table 1). The results suggested that multiple scatter correction gave the best data. When the best principle component score was 3, the sensitivity, specificity, and accuracy were all 1.

Figure 6 shows the scores of FM and MBM samples, which were separated into two groups. Thirty samples were predicted with 100 % accuracy using the PLS-DA model which was established based on multiplicative scatter correction pretreatment (Table 2).

## Identification of the FM and MBM Mixture

In order to identify the mixed FM and MBM samples and obtain their spatial distribution, we applied the threshold method to classify the images using a histogram searching technique. After obtaining the histogram, the spectral image was taken at 560 nm where both FM and MBM show peaks; however, the fluorescent intensities of the peaks are different.

**Table 1** Recognition rate of PLS-DA using different pretreatment methods

| Pretreatment method | Sensitivity | Specificity | Accuracy | Optimal component score |
|---|---|---|---|---|
| Original data | 0.982 | 0.91 | 0.95 | 4 |
| Standard normal transformation | 0.98 | 0.87 | 0.92 | 4 |
| First derivative | 0.94 | 0.87 | 0.90 | 8 |
| Second derivative | 1.00 | 0.88 | 0.92 | 5 |
| Multiplicative scatter correction | 1.00 | 1.00 | 1.00 | 3 |

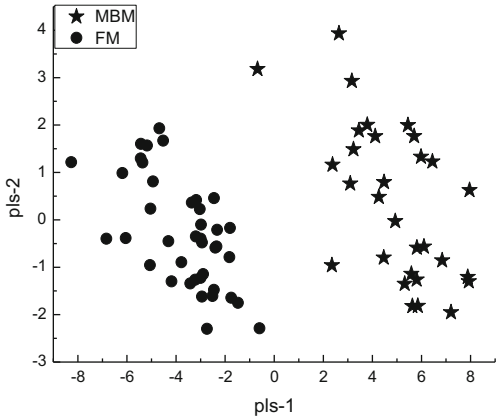


**Fig. 6** PLS-DA score distribution of principal components in tested samples

The spectral curves of FM and MBM were separated in the image.

As shown in the histogram (Fig. 7), there were two obvious valleys with grayscale values of 10 and 15, respectively. The curve disappeared at a grayscale value of 31; therefore, we concluded that there were two thresholds and three grayscale areas. The background grayscale area ranged from 0 to 10. The MBM grayscale area was from 10 to 15 according to the fluorescence intensity in the average spectrogram and is shown as the green areas. The FM grayscale area was at the 15–31 range and is displayed as the red areas. Three thresholds range was adopted to map the PC image, and the classification results are presented in Fig. 8.

The distribution of the upper and lower levels was considered the same because the tested powder was a thin layer. The frequency of each grayscale value at the two ranges was used for classification. The FM and MBM accounted for 52.6 and 47.4 % of the total volume, respectively, so the results were in agreement with the actual ratio. Furthermore, the spatial distribution of FM and MBM was observed visually in the PC image.

## LOD of the Method

Limit of detection (LOD) of the method means the minimum detectable concentration of the method. IUPAC (IUPAC,

**Table 2** Prediction results of PLS-DA modeling

| Actual value | Predicted value | |
|---|---|---|
| | Fish meal | Meat and bone meal |
| Fish meal | 14 | 0 |
| Meat and bone meal | 0 | 6 |
| Sensitivity | 1 | 1 |
| Specificity | 1 | 1 |
| Accuracy | 1 | 1 |

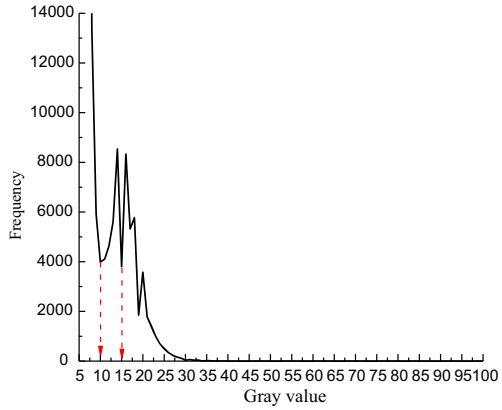


**Fig. 7** The histogram of the mixed powder of fish meal and meat and bone meal at 560 nm

1978) defined LOD as "the minimum measurement ($X_L$) that could be detected with reasonable reliability during a known (or given) analysis process. $X_L$ could be expressed by concentration ($C_L$) or quantity ($q_L$)."

$$X_L = \overline{X_0} + KS_0 \quad (2)$$

Where $\overline{X_0}$ is the mean blank measurement, $S_0$ is the standard deviation (SD) of blank measured value, and $K$ is a constant determined according to confidence level, which generally values 3. Hence, $C_L$ or $q_L$ could be calculated:

$$C_L(q_L) = X_L\text{-}X_0 \Big/ S = KS_0 \Big/ S \quad (3)$$

where $S$ is slope of the analyzed calibration curve. It is a constant under low concentration.

$X_L$ in the definition of IUPAC refers to indicating signal value of instrument. "Analysis Method" thinks that the result calculated from Equation (Cao Jijuan et al. 2003) is the LOD

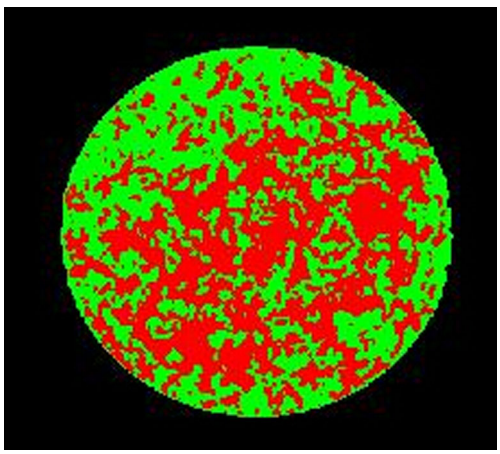

**Fig. 8** The classification results are indicated via the pseudo-color image of the mixed powder of FM and MBM

**Table 3** The statistical analysis results of standard deviation of concentration in repeated measurement process

| The percent content of MBM% | Standard deviation (%) |
|---|---|
| c[MBM]=1.5 % | 1.01 |
| c[MBM]=3 % | 1.27 |
| c[MBM]=5 % | 1.63 |

of the method. No agreement on how to measure and calculate LOD of the method directly has been reached yet. According to the definition of IUPAC, one reasonable way is to measure LOD of the method directly from known samples with approximately blank concentration. In the experiment, three low concentration-mixed powder samples were prepared in advance. The meat and bone meal (MBM) percentages in these three samples were c[MBM]=1.5 %, c[MBM]=3 %, and c[MBM]=5 %, respectively. Next, these three samples were detected by following to the image and spectra collection process (Image and spectrum acquisition). Each sample was tested 10 times and SD was calculated. Tested MBM percentages and SD are listed in Table 3.

A regression line of SD concentration was drawn from the statistical analysis results in Table 3. It can be known from Eq. (3) that there's a linear relationship between $S_0$ and $C_L$ (Fig. 9). Let $b$ be the intercept of the intersection point between the straight line and vertical coordinates. It is calculated that $b$=0.0075 according to the intersection point between the extending line and the vertical coordinates. This is the theoretical LOD of the method of MBM percentage in the mixed powder.

Therefore, all three samples present small SD. This reflects that the LLA of MBM percentage in the mixed powder detected in the experiment is c[MBM]=1.5 %. Moreover, theoretical LOD calculated from Table 3 is about c[MBM]= 0.75 %, indicating that the proposed method is reliable when

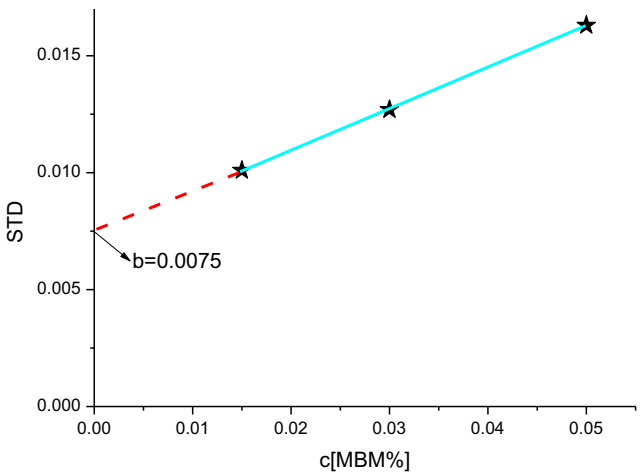


**Fig. 9** The linear regression line of standard deviation-concentration

measuring samples with higher than 0.75 % MBM percentage.

## Conclusion

In this study, we established a model to rapidly identify FM and MBM content based on the spectral and spatial information provided by an FSI approach. The PLS-DA method was used in the model, and the spatial distribution of FM and MBM was obtained from the resulting image. The feasibility of applying the FSI technique to the identification of FM and MBM was also investigated and the results suggest that the model worked best after multiplicative scatter correction where the sensitivity, specificity, and accuracy all equaled to 1. The findings indicate that it is feasible to identify FM and MBM via FSI.

In the experiment, FSI was thoroughly used for investigation by mixing the FM and MBM samples at a ratio of 1:1, by plotting the PC image based on the grayscale histogram, and by spatially identifying the mixed powder using the resulting PC image. The results showed that The FM and MBM accounted for 52.6 and 47.4 % of the total volume respectively, and the results were in agreement with the actual ratio (1:1). The spectral and spatial information provided by FSI can be used to identify FM and MBM rapidly and nondestructively as shown in the experiments.

**Acknowledgments** This work was supported by the Specialized Research Fund for the Doctoral Program of Higher Education of China (20124401120005), the Key Technologies R&D Program of Guangdong Province, China (2012A032300016), the Natural Science Foundation of Guangdong Province, China (S2011040001850), the Guangdong College of Outstanding Youth Innovation Talent Training Project in China (LYM11026), and the Fundamental Research Funds for the Central Universities, China (21612436 and 21612353). We also gratefully acknowledge many of our colleagues for their stimulating discussions in this field.

**Conflict of Interest** Yuanpeng Li declares that she has no conflict of interest. Furong Huang declares that she has no conflict of interest. Ruiyi Xian declares that he has no conflict of interest. Xiaoshu Lu declares that he has no conflict of interest. Jia Dong declares that she has no conflict of interest. Yong Wang declares that he has no conflict of interest. Xingdan Chen declares that he has no conflict of interest. Zhenqiang Chen declares that he has no conflict of interest. This article does not contain any studies with human or animal subjects.

## References

Cao J, Xing-an L, Gang W, Mingsheng C (2003) Method on PCR detection of bovine materials in animal feed stuffs. J Hyg Res 32(1):30–33

Castlcman KR (1998) (Translated by Zhu Zhi-gang, et al.). Digital image processing[M]. Electronic Industry Press, Beijing

Chen W-g (2003) The identification and detection methods of 1 adulterating fish 2 meal. J China Fish 12:66–67

Constantinou P, Dacosta RS, Wilson BC (2009) Extending immunofluorescence detection limits in whole paraffin-embedded formalin fixed tissues using hyperspectral confocal fluorescence imaging. J Microsc 234(2):137–146

Gendrin C, Roggo Y, Collet C (2007) Content uniformity of pharmaceutical solid dosage forms by near infrared hyperspectral imaging: a feasibility study. J Talanta 73:733–741

Hang W-x, Qi-chang A, Jing Z, Fu-bin L (2010) Self-adaptive region growing algorithm to segment images of spectral imaging for TCM assessment. J Appl Opt 31(1):78–83

Hao Y, Xudong S et al (2010) Application of visible and near infrared spectroscopy to identification of navel orange varieties using SIMCA and PLS -DA methods. J Trans CSAE 26(12):373–377

Heinzmann SS, Brown IJ, Chan Q, Bictash M, Dumas M-E, Kochhar S, Stamler J, Holmes E, Elliott P, Nicholson JK (2010) Metabolic profiling strategy for discovery of nutritional biomarkers: proline betaine as a marker of citrus consumption. American J Clin Nutr 92: 436–443

IUPAC (1978) Spectrochim Acta 23B(6):245

Liu Q (2006) Establishment of a sandwich ELISA for the detection of bovine and ovine MBM. [D]. Yangzhou University, Yangzhou of Jiangsu Province

Lv X, Li H, Wang J, Dong Y, Li J, Qin Y (2013) Quantification of fishmeal in compound feed using NIR spectroscopy. J Food Anal Methods 6(3):906–914

Ouyang A, Zhao Z (2013) Application of visible and near infrared spectroscopy to identification of lubricant oil using PLS-DA methods. J Chin Agric Mechanization 34(1):181–185

Peng Y-y, Xu-dong S, Yan-de L (2010) Research progress of hyperspectral imaging in nondestructive detection of fruits and vegetables quality. J Laser Infrared 40(6):586–593

Shi G-t, Lu-jia H, Zeng-ling Y, Xian L (2009) Methods of analyzing soybean meal adulteration in fish meal based on visible and near infrared reflectance spectroscopy. J Spectrosc Spectr Anal 29(2): 362–366

Wang Ji-qiang, Zhang Bo, Zhang Bao-tong, et al.(2012). The classification of fish meal, processing technology and quality control measures. J Feed wide-Angle. (15):25–27

Yang H (2006) Image segmentation threshold method research. J liaoning university 33(2):135–137

Yang Y (2010) Identify fish meal quality via physicochemical methods[J]. Guangdong Chem Ind 37(12):222–223

Yang J, Hai-feng D, Jun-ning F (2006) Methods for the detection of adulterated fish meal. Feed Ind 27(19):29–31

Zhan X-m, Lu-jia H, Xian L, Zeng-ling Y (2009) Genetic algorithm is used for predicting meat and bone meal content in fishmeal by near Infrared spectroscopy. J Acta Opt Sin 29(10):2800–2804

Zhang Y (1999) Image engineering (I) Image processing and analysis[M]. Tsinghua university press, Bei Jing

Zhang L, Xiao-ou S, Ping L, Bo S (2009) Detection of different original meat and bone meal in the concentrate supplementation of dairy cow diets by microscopy. Chinese J Anim Sci 45(10):62–64

Zhao J, Qi-chang P, Ji M et al (2010) Spectral imaging technology applied to mixed powder of Rhizoma coptidis and cortex Phellodendri chinensis. J Acta Opt Sin 30(11):3259–3264

Zhu Q, Huang M, Zhao X, Wang S (2013) Wavelength selection of hyperspectral scattering image using new semi-supervised affinity propagation for prediction of firmness and soluble solid content in apples. J Food Anal Methods 6(1):334–342